doi:10.1093/brain/awz021 BRAIN 2019: 142; 952–965 | 952

BRAIN
A JOURNAL OF NEUROLOGY

A probabilistic map of negative motor areas of the upper limb and face: a brain stimulation study

Fabien Rech,[1,2] Guillaume Herbet,[2,3] Yann Gaudeau,[4,5] Sophie Mézières,[6] Jean-Marie Moureau,[4,7] Sylvie Moritz-Gasser[2,3] and Hugues Duffau[2,3]

Negative motor responses (NMRs) are defined as movement arrests induced by direct electrical stimulation of the brain. The NMRs manifest themselves after the disruption of a corticosubcortical network involved in motor control, referred to as the 'negative motor network'. At present, the spatial topography of the negative motor areas (NMAs) is poorly known. Hence, the objectives of the present study were to establish the first probabilistic map of the NMAs of the upper limbs and face, identify potential subareas, and investigate the NMAs' relationships with the primary motor cortex. A total of 117 patients with low grade glioma underwent awake surgery with direct electrostimulation. The Montreal Neurological Institute coordinates of sites eliciting NMRs (face and upper limbs) were registered. A probabilistic map was created, and subareas were identified in a cluster analysis. Each cluster was then plotted on the Glasser atlas and the 1200 Subjects Group Average Data from the Human Connectome Project, in order to study connectivity and compare the results with recent parcellation data. We elicited 386 NMRs (mean $\pm$ standard deviation current intensity: 2.26 $\pm$ 0.5 mA) distributed throughout the precentral gyrus in both hemispheres. In each hemisphere, we found two clusters for facial NMRs. For upper limb NMRs, we found two clusters in the right hemisphere; and three in the left. Each cluster overlapped with parcellations from the Glasser atlas. For the face, the NMAs were associated with areas 55b and 6v. For the upper limbs, the NMAs were linked to areas 6v, 6d, and 55b. Each NMA cluster showed a specific pattern of functionally connected areas, such as the inferior frontal gyrus, supplementary motor area, parietal areas, and posterior superior temporal gyrus. The white matter pathways projecting to these subareas involved the frontal aslant tract and the frontostriatal tract—both of which are well known to be associated with NMRs. This study constitutes the largest series to date of NMRs mapped to the lateral surface of both hemispheres. Rather than being randomly distributed, the NMAs appeared to be well structured and corresponded to parcellations identified by functional neuroimaging. Moreover, the white matter pathways known to drive NMRs are also connected to regions encompassing NMAs. Taken as a whole, our results suggest that NMAs belong to a large-scale modulatory motor network. Our new probabilistic map might constitute a valuable tool for use in further clinical and fundamental studies of motor control.

1 Department of Neurosurgery, Central Hospital, CHRU Nancy, 29 avenue du Maréchal de Lattre de Tassigny, F-54000 Nancy, France
2 'Plasticity of Central Nervous System, Stem Cells and Glial Tumours' group, INSERM U1051, Institute for Neurosciences of Montpellier, F-34295 Montpellier, France
3 Department of Neurosurgery, Gui de Chauliac Hospital, Montpellier University Medical Center, 80 avenue Augustin Fliche, F-34295 Montpellier, France
4 Centre de Recherche en Automatique de Nancy, UMR 7039, Faculté de médecine, Université de Lorraine, F-54000 Nancy, France
5 Université de Strasbourg, 30 rue Maire Andre Traband, F-67500 Haguenau, France
6 Université de Lorraine, I.E.C.L., INRIA-BIGS, CNRS UMR 7502, F-54506 Vandoeuvre-les-Nancy, France
7 Centre de Recherche en Automatique de Nancy, UMR 7039, CNRS, Université de Lorraine, F-54000 Nancy, France

Received April 29, 2018. Revised December 2, 2018. Accepted December 14, 2018. Advance Access publication February 7, 2019

Correspondence to: Professor Hugues Duffau, MD, PhD
Department of Neurosurgery, Gui de Chauliac Hospital, CHU Montpellier
80 Avenue Augustin Fliche, F-34295 Montpellier, France
E-mail: h-duffau@chu-montpellier.fr

Keywords: negative motor area; awake surgery; electrical stimulation mapping; motor control; probabilistic map

Abbreviations: AF = arcuate fasciculus; FAT = frontal aslant tract; FEF = frontal eye field; FST = fronto-striatal tract; MPA = maximal probability area; NMA = negative motor area; NMR = negative motor response; PMR = positive motor response; SLF = superior longitudinal fasciculus; SMA = supplementary motor area

Introduction

Negative motor responses (NMRs) are defined as the complete inhibition of movement without the loss of muscle tone or consciousness, and are elicited by direct electrostimulation of the brain (Lüders *et al.*, 1987). Negative motor areas (NMAs) correspond to the cortical areas at which electrostimulation can induce an NMR of the face or upper or lower limbs, and are distributed across the medial and lateral surfaces of both hemispheres (Lüders *et al.*, 1995). However, the NMRs' functional significance remains poorly understood; in particular, it is not clear whether or not they have an inhibitory role (Filevich *et al.*, 2012). Recently, several studies showed that NMRs can also be elicited by stimulating the white matter under premotor areas (Schucht *et al.*, 2013; Rech *et al.*, 2014). As it was possible to identify NMRs at the cortical and the subcortical level, the existence of a network involved in motor control, called the 'negative motor network', was assumed. The white matter pathways subserving this network [namely the frontal aslant tract (FAT) and the frontostriatal tract (FST)] have been described (Kinoshita *et al.*, 2015; Rech *et al.*, 2016). Based on these findings, Rech *et al.* (2017) described the consequences of damaging part of the negative motor network on motor function, i.e. impairments of bimanual coordination and fine movements. Nevertheless, the cortical projections of the white matter tracts subserving the negative motor network, and the precise spatial distribution and coordinates of the cortical sites eliciting NMRs have not been investigated in detail. Furthermore, their relationships with the primary motor areas and others cortical and subcortical structures involved in motor control are still poorly known. As a consequence, and on the same lines as Penfield and Brodley's (1937) study of the primary motor cortex, we sought to describe for the first time the spatial distribution of cortical NMRs in 117 patients operated on for diffuse low grade glioma. We created a probabilistic map and identified clusters of responses corresponding to subparts of a broader corticosubcortical motor control network.

Patients and methods

Patients

The present study included adult patients treated for low-grade glioma at Gui de Chauliac Hospital (Montpellier University Medical Center, Montpellier, France) between 2012 and 2016. In a clinical examination, the neurosurgeon checked for possible neurological impairments in general and motor impairments in particular, since the latter constituted an exclusion criterion. All the patients were operated on under 'awake' conditions with functional brain mapping, and presented at least one brain site eliciting an NMR during electrical stimulation. All patients underwent a language assessment with a neuropsychologist and a speech therapist.

Each patient provided his/her informed consent prior to surgery. The study was conducted in accordance with our institution's ethical standards for a retrospective study. The stimulation mapping data were obtained during routine clinical practice and not as part of an experimental investigation. Our standard surgical approach includes awake craniotomy with direct electrical stimulation mapping. Patients consented to the retrospective extraction of clinical data from their medical records.

Cortical mapping

Each patient underwent the surgical resection of low grade glioma with intraoperative direct electrical stimulation mapping, as described previously (Duffau *et al.*, 1999). This procedure increases the quality of the resection while sparing functional networks and thus increasing the patient's quality of life (De Benedictis *et al.*, 2010).

A large bone flap was created to systematically expose the precentral gyrus and obtain positive mapping. After exposure of the brain, ultrasonography was used to determine the tumour boundaries. Next, electrical stimulation (60 Hz, biphasic, 1 ms pulse width; delivered for 4 s via a bipolar electrode with a tip-to-tip distance of 5 mm) was used to determine the functional boundaries. Patients were asked to count from 1 to 10 and to concurrently perform alternating flexions and extensions of the contralateral upper limb [all joints performing the same movement at the same time, i.e. the elbow (range: 0 to 90°), wrist and all fingers, with complete closure and opening of the hand, and while the shoulder remained at

rest] at a frequency of 0.5 Hz (i.e. one flexion-extension cycle every 2 s). The stimulation intensity was increased in 0.5 mA increments (from a baseline intensity of 1 mA to a maximum intensity of 4 mA) until speech arrest or a movement disorder (contraction/inhibition) was elicited. After determining the stimulation threshold, cortical mapping was initiated by delivering electrical stimulations at the same intensity over the whole exposed surface of the brain (and at least the precentral gyrus, tumour areas and peri-tumoural areas). These parameters were not modified during the cortical and subcortical mapping. Indeed, it was not mandatory to increase the stimulation intensity after finding the optimal threshold because this surgical protocol can be accomplished without inducing permanent impairments, i.e. by avoiding false-negative sites (Boetto *et al.*, 2015). Furthermore, increasing the intensity might lead to intraoperative seizures, greater current diffusion and thus false-positives, which might disturb the mapping.

Moreover, electrocorticography was not applied; a recent study showed that electrocorticography-free awake surgery for glioma is safe, reproducible, and associated with excellent functional and oncological outcomes. Furthermore, after-discharges occur mainly at intensities >4 mA (median: 6 mA) in the frontal lobe, which explains why maintaining a low stimulation threshold drastically reduces the incidence of these discharges. In fact, subcortical mapping is essential during tumour resection; it guides the resection along the fibres up to eloquent cortical areas, helps the surgeon to optimize the resection in cortical areas, and also sometimes enables supratotal resection with zero margins around crucial epicentres. This method allows the neurosurgeon to rule out false-positives caused by after-discharges (Boetto *et al.*, 2016).

For the mapping, the patient was asked to perform an object naming task (DO 80) (Metz-Lutz *et al.*, 1991) at the same time as the motor task described above. This dual task was monitored by a neuropsychologist or a speech therapist. A site was considered to be functional if (i) stimulation led to an impairment; and (ii) the cessation of stimulation led to normalization three times in a non-sequential manner (i.e. without stimulating the same site twice in succession).

With regard to motor function, we recorded NMRs and positive motor responses (PMRs). A PMR was defined as the contraction of a muscle or muscle group responsible for an involuntary movement (Penfield and Boldrey, 1937). An NMR was defined as the complete inhibition of movement without the loss of muscle tone or consciousness (Lüders *et al.*, 1987). The neuropsychologist or speech therapist checked whether the movement disorder was due to contraction or inhibition and, for inhibition, whether the movement was slowed down or interrupted despite the presence of muscle tone and consciousness. This assessment was performed for speech, the face, and the upper limbs.

Each response to electrical stimulation was identified by a sterile tag placed directly on the brain's surface. Resection was then performed until cortical and subcortical functional boundaries were identified. Photographs were taken before and after the resection for off-line data processing. The patient was anaesthetized, and the surgical site was closed.

Normalization and extraction of coordinates

The surgical protocol included preoperative MRI (acquired 1 day before surgery) and postoperative MRI (acquired 1 day and 3 months after surgery), including 1 mm isometric 3D T_1 sequences used for normalization, as described previously (Herbet *et al.*, 2016; Rech *et al.*, 2016). Briefly, each MRI dataset was first converted into the NIFTI format using MRIcroGL software (http://www.mccauslandcenter.sc.edu/mricrogl/). Next, the data were normalized with SPM12 (http://www.fil.ion.ucl.ac.uk/spm/software/spm12/), implemented in the MATLAB environment (version R2016a, The Mathworks, Inc., Natick, MA, USA). Anatomical landmarks (such as vessels and sulci on perioperative photographs, pre- and postoperative MRI) and surgical reports were used to determine the optimal location of electrical stimulation responses. Next, each response was plotted on a normalized 3D rendering template (the ICBM 152 asymmetrical template) with a 3 mm radius spherical volume of interest (VOI) in MRIcron (http://www.mccauslandcenter.sc.edu/crnl/mricron/). A 3 mm radius was chosen with regard to the electrode's tip-to-tip distance of the (5 mm). The Montreal Neurological Institute (MNI) coordinates (x, y, z) of each stimulation site (the centre of the spherical volume of interest) were extracted and recorded. Responses were then categorized as a PMR or an NMR in the right or left hemisphere, and as affecting the face, speech, or the upper limb.

Establishment of a probabilistic map

As described in the literature (Mandonnet *et al.*, 2007; Ius *et al.*, 2011; Herbet *et al.*, 2016), each stimulated voxel was binarized to a value of 0 (no response) or 1 (response) for each kind of response; this enabled us to generate a binarized map for each patient and each response. In a given patient, the value was set to 1 for all the voxels located on a site considered to be functional (i.e. after three stimulations eliciting the corresponding response in a non-sequential manner, as described above). Next, the probability with which a voxel elicited a specific kind of response was determined (using MRIcron software) from the ratio of the total number of patients in whom the voxel was functional and from the total number of times the voxel was stimulated (corresponding to the total number of patients operated on the same side). The following equation was then applied:

$$P = (V1 + V2 + \ldots + Vx)/n$$

where P is the probability of observing a given response, V is the value (1) of the voxel for the given response, x is the total number of times the voxel was considered to be functional, and n is the number of patients operated on for the same hemisphere. Brain shift and postoperative artefacts on MRI meant that it was not possible to precisely measure the exposed surface area of the precentral gyrus during the procedure. A probabilistic map was created by computing the binarized map and laying it over the ICBM 152 asymmetrical template, using MRIcroGL software for 3D surface rendering. Therefore, areas of stimulations could be displayed and not only the centre of the sphere.

Cluster analysis

The objective here was to establish whether NMRs over the precentral gyrus could be categorized into several subareas. For each kind of motor response, we performed a cluster analysis using MATLAB, as previously described (Tate *et al.*, 2014; Herbet *et al.*, 2016). The number of clusters was determined by applying the k-medoid algorithm to the centre of each volume of interest—enabling one to plot the centroid on the surface of the brain. The optimal number of clusters was determined with two distinct methods: the Davies Bouldin algorithm (Davies and Bouldin, 1979) and the average silhouette method (Rousseeuw, 1987) by varying the number of clusters from 2 to 10. Stimulation points were grouped into their respective clusters, and results were carried over onto the ICBM 151 asymmetrical template. The probability with which each cluster elicited an NMR was calculated by dividing the number of patients who presented at least one NMR in the cluster by the number of patients operated on the same side.

For each cluster, a map was created to determine the probability with which each voxel in the cluster elicit the associated response. The probability was calculated by applying the equation described above.

Comparison with an atlas

Our method generated several clusters for each kind of NMR. We sought to compare these results with previous parcellations of the precentral gyrus. To this end, we used the Glasser atlas (Glasser_et_al_2016_HCP_MMP1.0_6, from https://balsa.wustl.edu/sceneFile/show/Zvk4) because its parcellation map is built on structural, connectivity and functional data (from task-based and resting state-based functional MRI) (Glasser *et al.*, 2016). The Glasser atlas describes multiple functional areas inside the precentral gyrus, and so we matched our clusters with the atlas's parcellations. As both methods have different sources of functional data, we reasoned that a comparison of the respective areas might provide valuable information on the functional organization of the precentral gyrus. Therefore, using the Connectome Workbench (https://www.humanconnectome.org/software/connectome-workbench), each cluster of NMRs was overlapped on the Glasser atlas, and its border and centroids were plotted over the brain template. It was then possible to determine which areas (if any) of the Glasser map matched with a given cluster.

Functional connectivity analysis

Each cluster's functional connectivity was analysed against the 1200 Subjects Group Average Data from the Wu-Min HCP Data dataset (Van Essen *et al.*, 2012) downloaded from the Connectome database (Marcus *et al.*, 2011). Use of the Connectome Workbench enables one to assess the functional connectivity of a chosen region by plotting a seed on it. One seed was set per cluster; given that a cluster could overlap with two or more areas, the best seed location was calculated. The seeded area was chosen from among the parcellations that overlapped with the cluster. Next, the maximum probability area (MPA) was checked, along with the centroid's position. When the MPA and centroid were at the same position, the seed was plotted at that location. If there was a mismatch between the MPA and the centroid, the MPA was chosen as the seed location. When there was more than one MPA, the centroid position was chosen as the seed location if it matched with an MPA. If centroid was located outside MPAs, seeds were tested on each MPA.

White matter pathways

To highlight the neural networks associated with the NMRs and better understand the results of the functional connectivity analysis, we looked at which association pathways might emanate from each area harbouring a cluster. To this end, we used a recent tractography-based atlas (Rojkova *et al.*, 2016) that provides cortical projections of white matter tracts. Each cluster or association pathway connected to the precentral gyrus was plotted on a 3D brain template using MRIcroGL, in order to analyse the overlapping areas and the functional connectivity. Moreover, the relationships between clusters and projection pathways known to be involved in the negative motor network were also analysed. Lastly, we identified the cortical terminations that overlapped (partially or totally) with the clusters, in order to determine whether the latter constituted part of or all of a tract.

Data availability

Anonymized data will be shared by request from any qualified investigator.

Results

A total of 117 patients were included in the study. The characteristics of the patients and tumours are summarized in Table 1. The most common tumour sites were frontal (45.30%), frontotemporo-insular (19.66%), and temporal (17.09%). No permanent impairments were observed at 3 months after the surgery.

A total of 527 sites were documented on the lateral surface of the brain [mean ± standard deviation (SD) per brain: 4.50 ± 2.2 sites]. In all, there were 386 NMRs (accounting for 73% of all responses) and 141 PMRs (27% of all responses) (Table 2). The NMRs were equally distributed over the two sides of the brain (right: 34.9%; left: 38.3%), as were the PMRs (right: 14.6%; left 12.1%) (Fig. 1).

Positive motor responses

The PMRs were distributed over on the precentral gyrus, on the lateral surface of the hemisphere. Facial PMRs were located in and around the primary motor area of the face (Fig. 1). Upper limb PMRs were located more dorsally, i.e. in and around the hand knob corresponding to the primary motor area for the upper limb and the hand (Fig. 1). However, the areas associated with PMRs in both hemispheres extended outside the primary motor cortex. The distribution of PMRs throughout the motor and premotor areas has been described in detail elsewhere (Penfield and Boldrey, 1937; Duffau *et al.*, 2003; Mikuni *et al.*, 2006; Tate *et al.*, 2014; Borggraefe *et al.*, 2016).

Negative motor responses

The NMRs were distributed across the precentral gyrus (Fig. 1), as previously described (Mikuni *et al.*, 2006; Filevich *et al.*, 2012; Tate *et al.*, 2014). Interestingly, NMRs were more frequently elicited at a similar mean intensity (2.26 ± 0.5 mA for NMRs, and 2.2 ± 0.4 mA for PMRs) (Table 2). For a given patient, the NMRs were always situated more rostrally than the PMRs.

On both hemispheres, facial NMRs were distributed over the precentral gyrus (from the sylvian fissure to the superior frontal sulcus; Fig. 2). Stimulation of these sites elicited speech arrest. Given the surgical conditions (i.e. time constraints), the goal of the mapping was to rapidly identify functional boundaries for tumour resection (Duffau *et al.*, 1999). Consequently, when speech arrest was elicited, it was not possible to perform another task—moving the tongue to distinguish between a pure 'facial' NMR from a 'speech arrest' NMR, for example. Facial NMRs were elicited over the precentral gyrus on both hemispheres in a high proportion of patients (94.34% for the right and 89.06% for the left; Table 3). Only one facial NMR was observed for the (left) pars opercularis; the inferior frontal gyrus was invaded by the tumour in only 12% of cases and the pars opercularis stimulated in 82% of cases (Supplementary Tables 1 and 2). Seven stimulations of the retrocentral gyrus elicited face NMRs. For each hemisphere, two clusters were identified. The first one (cluster A, Fig. 3) extended over the precentral gyrus from the superior frontal sulcus to the inferior frontal sulcus, and overlapped with areas 55b and 6d from the Glasser parcellation. Its centroid was located at the junction between areas 55b and 6v on the left hemisphere, and between area 55b and the frontal eye field (FEF) on the right hemisphere. The maximum probability of finding a facial NMR in this cluster was situated at the junction between areas 6v and 55b on the left hemisphere (15%), and within area 55b on the right hemisphere (12%), rostrally to the face primary motor cortex. Considering the data on the cluster border, the maximum probability, and the centroid position as a whole, there was a good match between cluster A and area 55b.

The second cluster (cluster B, Fig. 3) was located more ventrally, in the ventral premotor cortex; this corresponded to area 6v in the Glasser parcellation. The MPAs were found dorsally and ventrally on the right (26%) but were less extensive on the left (29%). Centroids were located ventrally to area 6v to the same extent on both hemispheres. Therefore, area 6v matched well with cluster B, and was chosen as the seeding site.

Upper limb NMRs were distributed from the sylvian fissure to the hand knob (Fig. 4). They were located rostrally to the primary motor cortex. As had been seen for facial NMRs, there was a high frequency of upper limb NMRs over the precentral gyrus (95.31% for the left hemisphere and 100% for the right) (Table 2). Seven stimulations over the retrocentral gyrus elicited NMRs.

Two clusters were found on the right hemisphere (Fig. 5). One cluster (cluster A, Fig. 5) was located below the inferior frontal sulcus, and corresponded to areas 43 and 6v and part of area 55b in the Glasser parcellation. Its centroid was located in the postero-inferior part of area 6v. MPAs (P = 16%) were broadly distributed on both sides of the border between areas 6v and 55b. Therefore, centroid position was used to determine the seed and area 6v was chosen. The second cluster (cluster B, Fig. 5) overlapped with areas 6d and 55b and the FEF in the Glasser

Table 1 Characteristics of population and tumour

Population	
Patients, *n*	117
Age, years, mean ± SD	39 ± 10
Male:female ratio	0.95
Handedness	
Right	84.62%
Left	11.97%
Ambidextrous	3.42%
Tumour side	
Right	45.30%
Left	54.70%
Contralateral to handedness	52.99%
Tumour location	
Frontal	45.30%
Fronto-temporo-insular	19.66%
Parietal	11.11%
Temporal	17.09%

Table 2 Characteristics of stimulation sites

	Negative motor responses		Positives motor responses	
Current intensity, mA, mean ± SD	2.26 ± 0.5		2.2 ± 0.4	
Overall response proportion (*n* = 527)	73.24% (*n* = 386)		26.76% (*n* = 141)	
	Right: 34.91% (*n* = 184)	Left: 38.33% (*n* = 202)	Right: 14.61% (*n* = 77)	Left: 12.14% (*n* = 64)
Detailed response rate				
Face/speech arrest	39.85% (*n* = 210)		16.51% (*n* = 87)	
Upper limb	33.40% (*n* = 176)		10.25% (*n* = 54)	

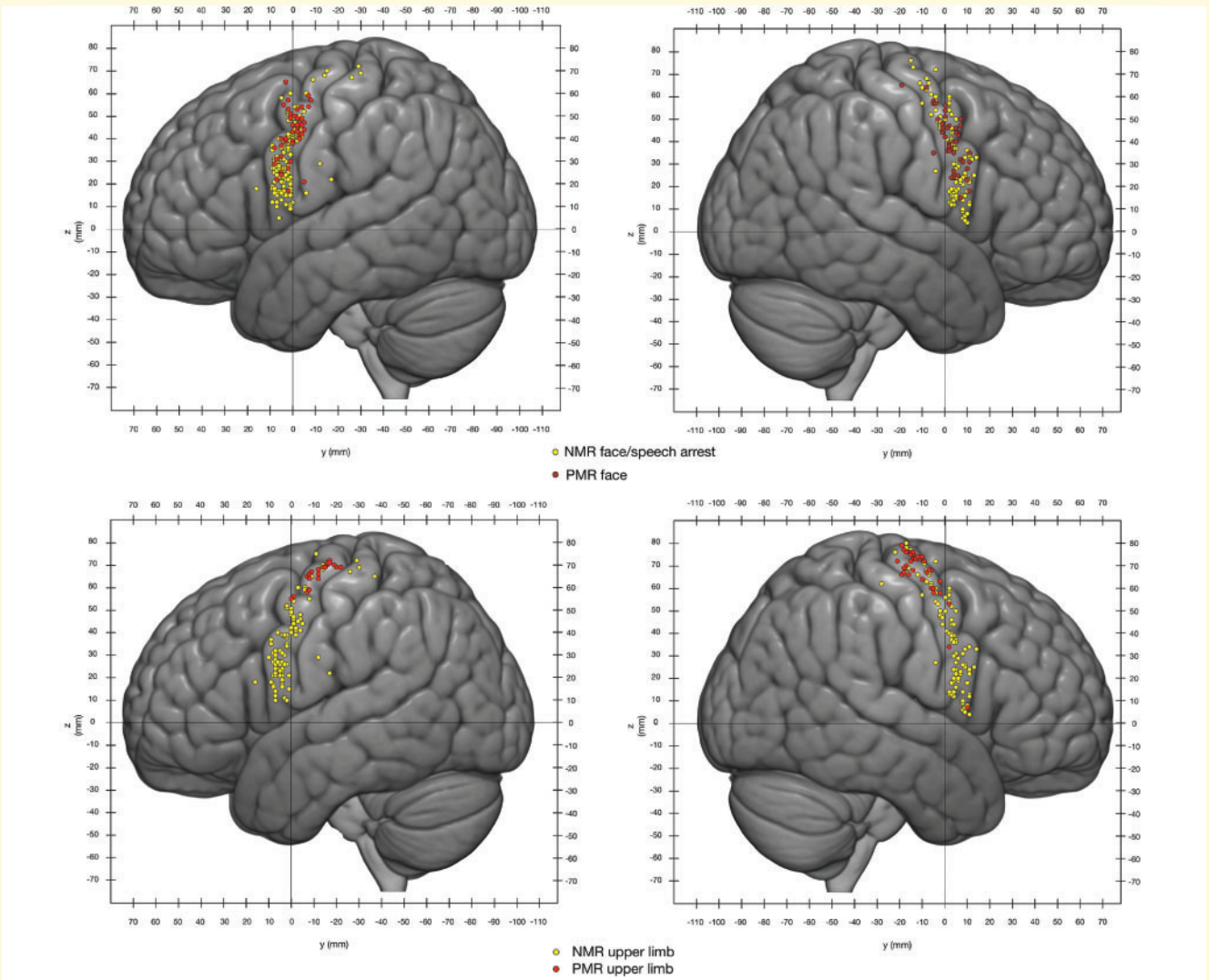

Figure 1 Overlap between NMRs and PMRs. Yellow dots = NMRs; red dots = PMRs. The coordinates correspond to the MNI reference space. The dot diameter has been reduced to 2 mm to make it easier to see all the stimulation sites.

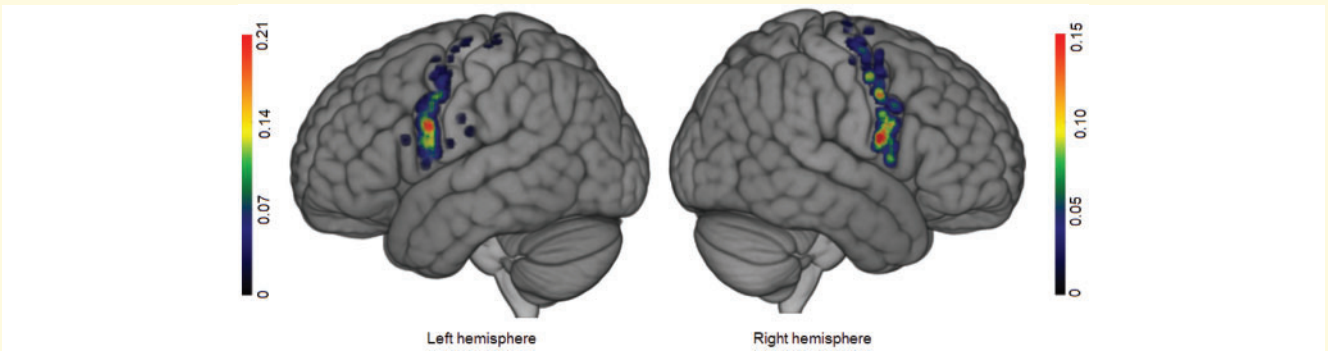

Figure 2 Probabilistic map of face/speech arrest NMRs for each hemisphere. The colour bar indicates the probability. Scales were adjusted for each hemisphere, to highlight differences inside the precentral gyrus.

Table 3 Probability of negative motor responses for each cluster and hemisphere

Response	Right hemisphere	Left hemisphere	Overall
Face/speech arrest	94.34%	89.06%	91.45%
Cluster A	37.74%	45.31%	
Cluster B	71.70%	70.31%	
Upper limb	100.00%	95.31%	95.8%
Cluster A	71.70%	54.69%	
Cluster B	39.62%	12.5%	
Cluster C		39.06%	

This table shows the overall probability for each hemisphere to elicit a negative motor response and the probability for each cluster in its hemisphere.

parcellation. The MPA (P = 11%) was located over areas 55b and 6d, and the centroid was located at the junction between the ventral part of area 6d and FEF. Thus, two seeds were used: one over area 55b, and another over area 6d.

Three clusters were found on the left hemisphere. Cluster A (Fig. 5) was located below the inferior frontal sulcus, and corresponded to all of area 6v and parts of areas 43 and 44. Its centroid was located inside the MPA (P = 20%) in the middle of area 6v, giving the seed location. Cluster B (Fig. 5) was located rostrally to primary motor cortex for the upper limbs and hands, and overlapped within area 6d. The associated MPA (P = 4%) was located at the junction between the FEF and area 6d, whereas the cluster's centroid

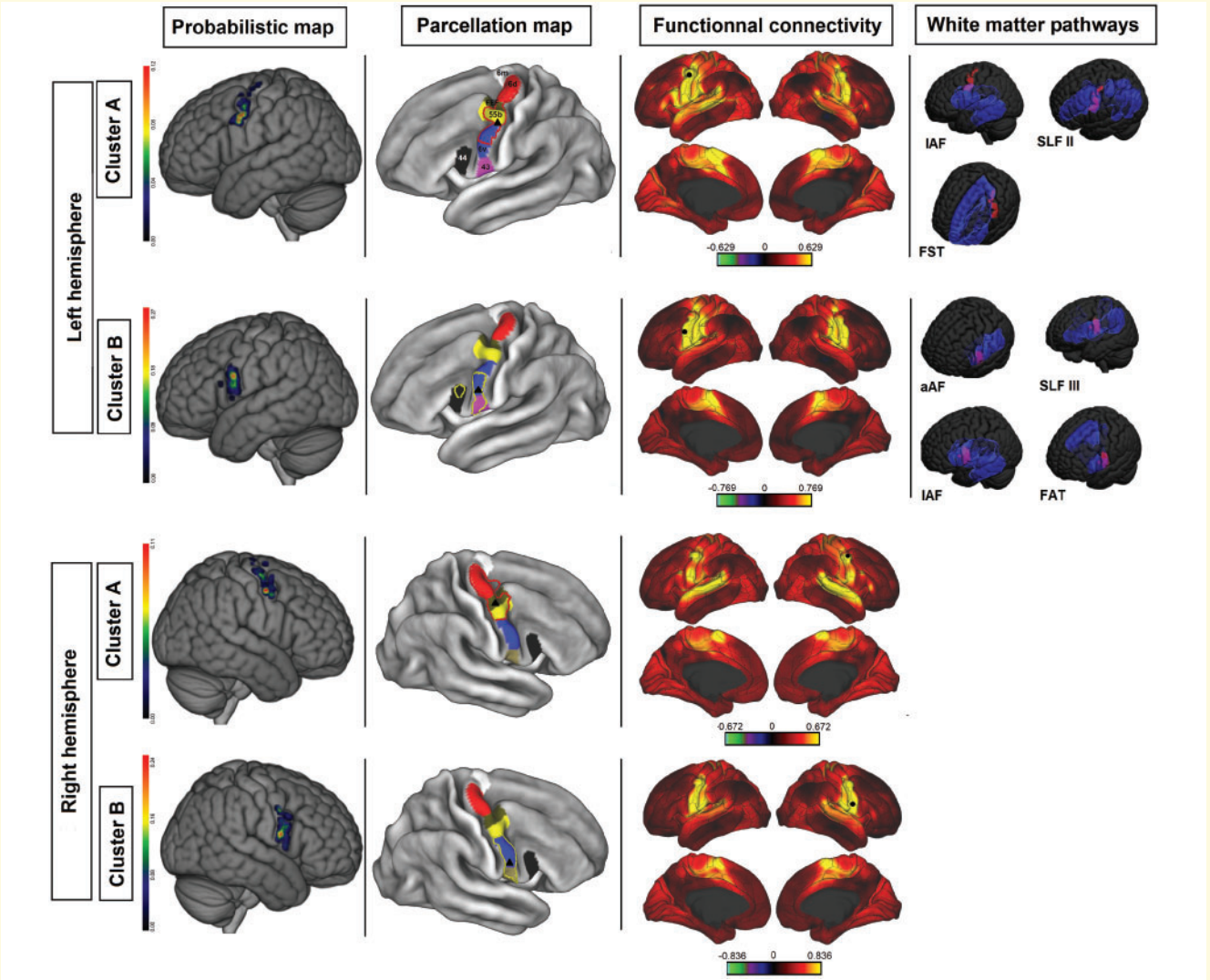

Figure 3 Cluster analysis of face/speech arrest NMAs. Each row corresponds to a cluster. First column: a probabilistic map of the cluster (colour bar scales were adjusted to highlight differences inside the precentral gyrus). Second column: overlap between the cluster boundaries (cluster A = red dots; cluster B = yellow dots) and the Glasser parcellation map (area 6 m = white; area 6d = red; FEF = brown; area 55 = yellow; area 6v = blue; area 43 = purple; area 44 = black; black triangle = centroid). Third column: areas functionally connected to the corresponding cluster, according to the Wu-Min HCP Data dataset (high connectivity = yellow; low connectivity = red; the colour bar represents Pearson's r; seed = black circle; Glasser parcellation map = black line). Fourth column: overlap (purple) between clusters (red) and white matter pathways (opaque blue = cortical projection; transparent blue = subcortical fibres).

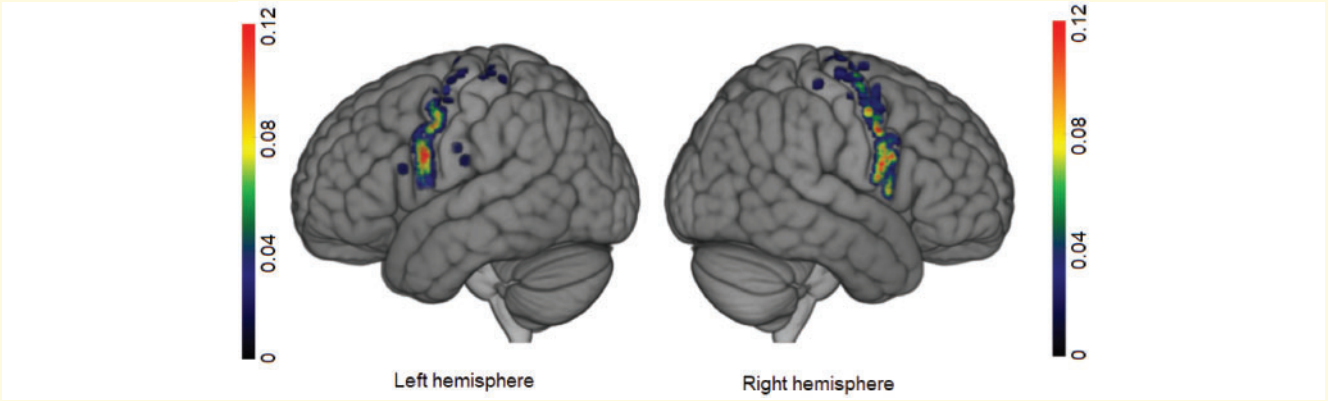

Figure 4 Probabilistic map of upper limb NMRs for each hemisphere. The colour bar indicates the probability. Scales were adjusted for each hemisphere, to highlight differences inside the precentral gyrus.

was located in the centre of area 6d. The seed was placed over the MPA, in area 6d. Cluster C (Fig. 5) was located between clusters A and B (rostrally to the face's primary motor area), and covered all of area 55b and the upper part of area 6v. The cluster centroid and the MPA ($P = 14\%$) straddled the boundary between areas 6v and 55b. The seed was placed in area 55b, at the border between areas 55b and 6v.

Functional connectivity

Our clustering (based on electrical stimulation) provided functionally segregated areas that overlapped with the Glasser parcellation. Establishing the same map with a different technique reinforces Glasser *et al.*'s results. As explained above, we were able to associate each cluster with a cortical area of the Glasser parcellation on the basis of the MPA, the centroid position and the cluster border. We then analysed each cluster's functional connectivity (Figs 3 and 5).

Face cluster A was correlated with area 55b, whereas face cluster B was located more ventrally and was associated with area 6v. The upper limb cluster A matched with area 6v. On the right hemisphere, the upper limb cluster B was distributed dorsally over areas 55b and 6d. On the left hemisphere, the upper limb cluster B was restricted to area 6d, and cluster C overlapped with area 55b.

Accordingly, three main areas (6v, 6d and 55b) emerged from our results and were used as seeds in the functional connectivity analysis, as described above. The functional connectivity analysis revealed that area 55b was connected ventrally with area 6v, the inferior frontal gyrus, and the superior temporal gyrus, dorsally with area 6d, posteriorly with the primary motor cortex and the retrocentral gyrus, and medially with the pre-supplementary motor area (preSMA) and the cingulate gyrus.

Area 6v was functionally connected posteriorly with the primary motor cortex and the retrocentral gyrus, dorsally with the superior parietal lobule and area 6d, and medially with the cingulate gyrus and the SMA.

Area 6d was connected posteriorly to the primary motor cortex the retrocentral gyrus and the parietal lobe, and medially to the cingulate gyrus.

White matter pathways

Several tracts are known to project fibres to the precentral gyrus and therefore to areas corresponding to the clusters found in the present study (Makris *et al.*, 2005; Catani *et al.*, 2012; Martino *et al.*, 2013). We used Rojkova's atlas to determine which white matter tracts might be connected to the negative motor network. The long branch of the arcuate fasciculus (lAF) and the anterior arcuate fasciculus (aAF), the superior longitudinal fascicle II (SLF II) and III (SLF III), the FST, and the FAT were identified as white matter pathways of interest because they all project to the NMAs on the precentral gyrus. In Rojkova's atlas, these pathways overlapped fully or partially with our clusters.

Face cluster A overlapped with the projections of the lAF, SLF II, and FST, while face cluster B overlapped with the projections of the aAF, SLF III, lAF, and FAT.

Upper limb cluster A overlapped with the cortical terminations of the lAF, aAF, and FAT. Cluster B matched the cortical projections of the FST and SLF II. Lastly, cluster C overlapped with the projections of the SLF II, lAF and aAF.

Discussion

The spatial distribution and underlying connectivity of negative motor responses

The spatial distribution of NMRs has long been a topic of interest (Penfield and Boldrey, 1937; Lüders *et al.*, 1987, 1995; Filevich *et al.*, 2012; Tate *et al.*, 2014; Borggraefe *et al.*, 2016). However, comparisons between studies are complicated by the lack of a robust set of coordinates (Filevich *et al.*, 2012). The present study is the first to

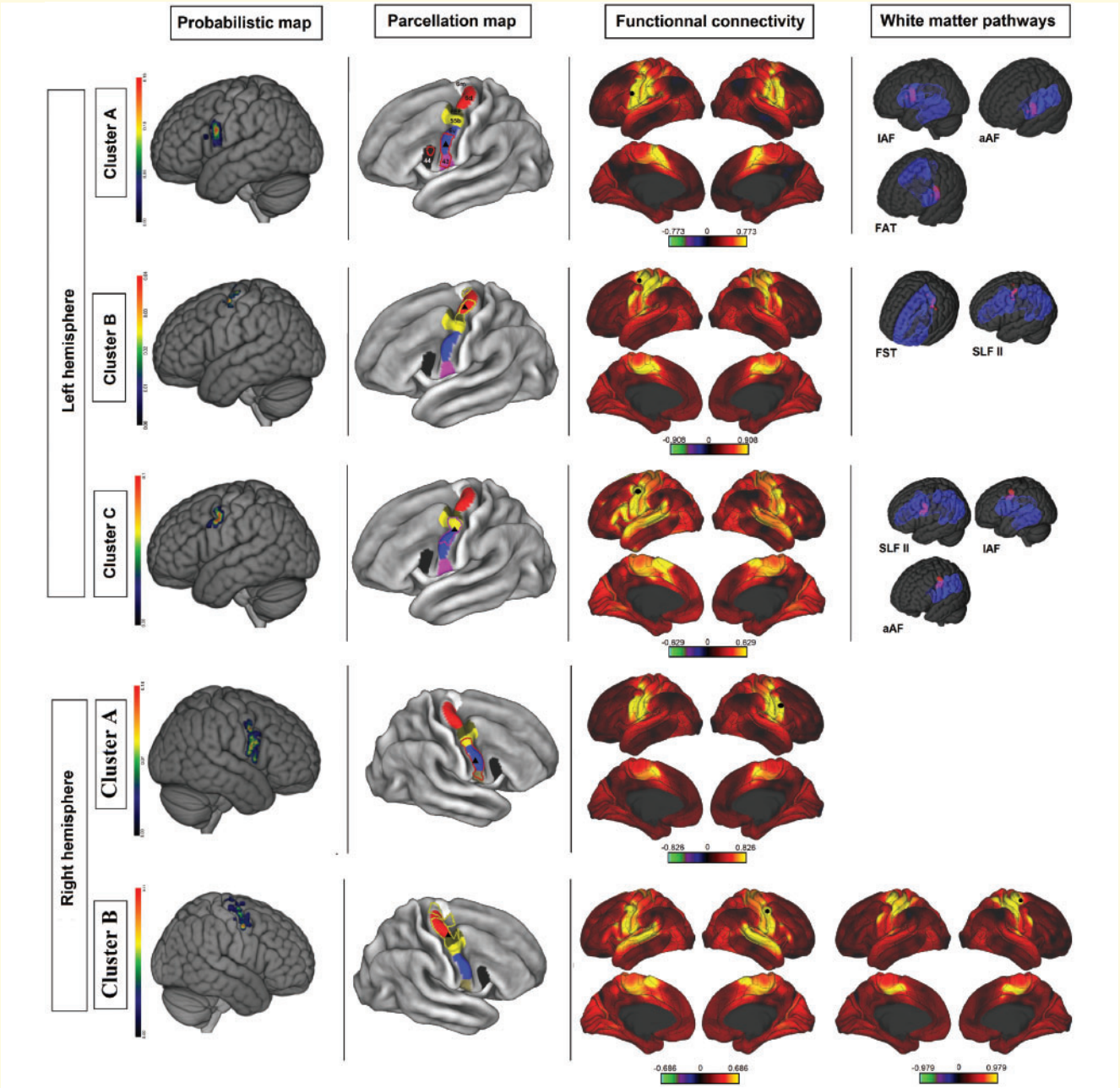

Figure 5 Cluster analysis of upper limb NMAs. Each row corresponds to a cluster. First column: probabilistic map of the cluster (colour bar scales were adjusted to highlight differences inside the precentral gyrus). Second column: overlap between cluster boundaries (cluster A = red dots; cluster B = yellow dots; cluster C = purple) and the Glasser parcellation map (area 6 m = white; area 6d = red; FEF = brown; area 55b = yellow; area 6v = blue; area 43 = purple; area 44 = black; black triangle = centroid). Third column: areas functionally connected to the corresponding cluster, according to the Wu-Min HCP Data dataset (high connectivity = yellow; low connectivity = red; the colour bar represents Pearson's r; seed = black circle; Glasser parcellation map = black line). Fourth column: overlap (purple) between clusters (red) and white matter pathways (opaque blue = cortical projection; transparent blue = subcortical fibres).

provide a probabilistic map of the cortical NMAs (based on the analysis of the spatial distribution of the NMRs) on the lateral face of the hemispheres in 117 patients. In all cases, the mapping protocol was based on intraoperative direct electrical stimulation. Our 3D probabilistic map of NMAs might be of value in further clinical and fundamental studies of movement and movement disorders.

First, the spatial distribution observed here was in agreement with previous reports (Mikuni *et al.*, 2006; Filevich *et al.*, 2012; Enatsu *et al.*, 2013; Tate *et al.*, 2014; Borggraefe *et al.*, 2016). In our study, however, NMRs were more elicited frequently (mean number of NMRs per patient: 3.3) and at lower stimulation intensities (mean: 2.26 ± 0.5 mA) than in the literature (range: 5 to

15 mA) (Lüders *et al.*, 1987, 1995; Enatsu *et al.*, 2013; Borggraefe *et al.*, 2016). We found that facial NMRs (right: 94.34%; left: 89.06%) and upper limb NMRs (right: 100%; left: 95.31%) were most frequently elicited. Consequently, our study provided a unique, reproducible, homogeneous dataset about NMRs that is amenable to cluster analysis. Our analysis is the first to show that NMRs are neither distributed widely (in contrast to previous suggestions of a lack of precise organization on the hemisphere's lateral surface) (Mikuni *et al.*, 2006; Filevich *et al.*, 2012; Borggraefe *et al.*, 2016) nor somatotopically localized over the inferior frontal gyrus (Lüders *et al.*, 1995); in fact, we found that NMRs were grouped into several areas over the precentral gyrus. Brain plasticity cannot be responsible for the fact that only one NMR was found over the inferior frontal gyrus, since the latter was invaded by the tumour in only 12% of cases. Moreover, previous studies did not report NMRs over the inferior frontal gyrus (Mikuni *et al.*, 2006; Borggraefe *et al.*, 2016).

Concerning face NMRs, our cluster analysis revealed two epicentres: one in area 6v, and the other in area 55b. First, cluster B (in area 6v) appeared to be connected to the SMA, which is consistent with the frontal aslant tract connecting the posterior region of the inferior frontal gyrus and the precentral gyrus to the SMA (Catani *et al.*, 2012). Moreover, stimulation of the FAT can generate speech arrest (Kinoshita *et al.*, 2015), as can stimulations of the SMA (Lüders *et al.*, 1987; Filevich *et al.*, 2012). This cluster is probably also connected at a subcortical level to the retrocentral gyrus by frontoparietal loop-driving NMRs (Almairac *et al.*, 2014). Second, cluster A was more broadly distributed but the locations of the MPA and the centroid tend to highlight area 55 b. This might mean that cluster A was connected to the inferior frontal gyrus, the superior temporal gyrus, the SMA, the preSMA, and the face representation of the primary motor cortex—a larger network than for cluster B.

Upper limb NMRs also showed specific epicentres. On the right hemisphere, cluster A was located over the ventral premotor cortex and appeared to be connected to the SMA, the primary motor cortex, the dorsal premotor cortex and retrocentral gyrus. Cluster B was rostral to the primary motor cortex for the upper limb, and corresponded to area 6d (which is equivalent to the dorsal premotor cortex). Dorsal and ventral premotor cortex are connected both to each other and to the primary motor cortex, as shown in the functional connectivity map (Fig. 5) and as previously described in a non-human primate (Dum, 2005). On the left hemisphere, a third cluster (cluster C) emerged from our analysis; it was located on area 55b, and overlapped partly with area 6v and the FEF. The overall distribution of the upper limb NMRs in both hemispheres is the same. Interestingly, the third upper limb cluster was located in the left hemisphere within a region (area 55b) with connections to many other areas. It is noteworthy there was a difference between left- and right-handed patients with regard to the probability of eliciting an NMR in this cluster ($P = 12.5\%$ for left-handed patients and 42.8% for right-handed patients). However, this difference was not statistically significant—probably as a result of the small number of left-handed patients. Since handedness might be due to asymmetric connections between the primary motor cortex and dorsal premotor cortex (as shown in resting state MRI experiments) (Pool *et al.*, 2015), we hypothesize that the asymmetry observed in our study might also be related (at least in part) to handedness.

Understanding the role of the negative motor network

The axonal connectivity mediating the negative motor network has been recently described (Schucht *et al.*, 2013; Almairac *et al.*, 2014; Rech *et al.*, 2014, 2016, 2017; Kinoshita *et al.*, 2015). Although we are starting to understand the subcortical pathways underpinning motor control, very little is known about these pathways' cortical projections. Two main tracts are thought to be responsible for NMRs in the frontal lobe: the FAT and the FST (Kinoshita *et al.*, 2015) (Figs 3 and 5). The FAT connects the precentral and inferior frontal gyrus to the SMA, whereas the FST connects the precentral gyrus to the basal ganglia. The NMRs show a somatotopic distribution (Rech *et al.*, 2016). Nevertheless, our present study shows that the distribution of the NMRs over the precentral gyrus is far more complex; despite a broadly somatotopic distribution (face/ventral, upper limb/dorsal), some of the face and upper limb NMA clusters are intermingled. Thus, cortical projections from the FAT and the FST cannot alone account for the subcortical connectivity, since they do not completely overlap with the NMAs. Consequently, other white matter pathways might be involved, such as the lAF, aAF, and SLF. Moreover, intragyral tracts connecting the NMAs to the primary motor cortex and somatosensory areas might also be involved. Interestingly, some clusters only partially overlapped with white matter tracts; this might mean that the segregation could be greater in these clusters. Conversely, various subparts of a tract can project to different clusters, which might account for inter-cluster plasticity for clusters targeted by the same white matter pathways (Mikuni *et al.*, 2006; van Geemen *et al.*, 2014). In future multimodal imaging studies, our probabilistic map might help researchers to better understand the white matter tracts that subserve motor control in this region.

The role of the negative motor responses

The NMAs' role—and particularly whether they have an inhibitory function—remains subject to debate. Some researchers assume that electrical stimulation disrupts sites with a positive motor function, whereas other researchers consider that NMAs inhibit motor control (Chauvel *et al.*, 1996; Filevich *et al.*, 2012). Our present results showed

that at the cortical level, NMRs could be elicited all over the precentral gyrus at a lower stimulation intensity than in previous series (Lüders *et al.*, 1987, 1995; Enatsu *et al.*, 2013; Borggraefe *et al.*, 2016), whereas PMRs (elicited at similar stimulation intensities) were frequently located immediately in front of the central sulcus. At the subcortical level, NMRs can also be elicited by stimulating the white matter tracts connected to the NMAs (Schucht *et al.*, 2013; Rech *et al.*, 2014, 2016)—corresponding here mainly to the FAT and the FST (Figs 3 and 5) (Kinoshita *et al.*, 2015). Given that these bundles are located in front of the pyramidal tract that emerges from the PMR, our results suggest that (i) the cortico-subcortical negative motor network has an inhibitory role *per se*; and (ii) PMRs are not artificially disrupted through intracortical inhibitory connections. In fact, the latter mechanism is very unlikely during direct stimulation of the axonal fibres emerging from the cortical NMAs, which are anatomically distinct from the pyramidal fibres (Schucht *et al.*, 2013).

The role of the dorsal and ventral premotor cortices in grasping and reaching are well known (Chouinard and Paus, 2006; Takahashi *et al.*, 2017). These areas are also involved in internally and externally driven movements—notably thanks to connections between premotor and parietal areas (Ariani *et al.*, 2015). Both areas contain representations of the arms and hands (He *et al.*, 1993), and are connected to each other and to the primary motor cortex (Dum, 2005; Catani *et al.*, 2012). Our results show that clusters of NMAs are located on the dorsal and the ventral premotor cortex, and that these clusters might be functionally connected to the primary motor cortex and the parietal lobe. Hence, these clusters of NMAs might have a role in the control of arm and hand movements during reaching and grasping and in internally or externally driven movements.

Moreover, the NMA sites correspond to those associated with the mirror neuron system (Buccino *et al.*, 2004; Cattaneo and Rizzolatti, 2009; Rizzolatti and Sinigaglia, 2016), namely the dorsal and the ventral premotor cortex. Furthermore, the cluster located over area 55b appears to be functionally connected to structures like the inferior frontal gyrus and the superior temporal gyrus, which are well known components of the mirror neuron system (Rizzolatti and Sinigaglia, 2016). Interestingly, a mechanism for action suppression involving the ventral premotor cortex's mirror properties has been suggested in the macaque (Kraskov *et al.*, 2009). Along the same lines, we hypothesize that NMAs play a role in inhibiting self-movement during action observation in humans.

The value of a probabilistic map of negative motor areas in neurosurgery, neurology and neuroscience

Detailed knowledge of the cortical organization of a network of NMAs might help the neurosurgeon to plan the surgical procedure. It might also facilitate brain mapping during tumour and epilepsy surgery. Indeed, cortical mapping of the negative motor network could be performed first in the MPAs, with a view to finding NMAs more quickly. Detection of the negative motor control network is essential for preserve fine motor skills during lesional surgery in and around the precentral gyrus. This argues for mandatory awake mapping to identify NMAs, regardless of the lesion's side and patient's handedness. Furthermore, the identification of new epicentres within the negative motor network (such as the extra-frontal areas connected to the precentral NMAs) suggests that one should be cautious regarding motor function during awake surgery in brain regions other than the premotor areas. This probabilistic map also adds new decisional components that can be discussed with the patient and his/her family before surgery (e.g. the 'oncofunctional ratio': the balance between more complete tumour resection and the risk of subtle motor impairments) (Duffau and Mandonnet, 2013).

Our probabilistic map might also be useful in understanding the pathophysiology of movement impairments and predicting recovery in brain-damaged patients based on the injured subareas; this has already been demonstrated for the subcortical part of the negative motor network (Rech *et al.*, 2017). In the same field, our atlas could be used to determine which area should be targeted during non-invasive brain stimulation, in order to prevent an imbalance between the primary motor cortices and to facilitate rehabilitation (Takeuchi *et al.*, 2005; Bradnam *et al.*, 2013).

Moreover, our atlas might help to provide a better understanding of the neural network subserving the cortical motor system control and the latter's connections with deep subcortical structures like the basal ganglia. The ability to use electrical stimulation to interrupt movement without loss of consciousness or muscle tone might open new perspectives for treating movement disorders and perhaps identifying new targets for brain stimulation.

From a more fundamental viewpoint, our probabilistic map provides a unique dataset with regard to the cortical origins of the so-called modulatory motor network (Schucht *et al.*, 2013; Rech *et al.*, 2014, 2016). The NMAs identified in this study could be used as regions of interest for exploring the motor control network's functional and structural connectivity (e.g. by using task-based or resting state functional MRI and tractography).

Limitations

Some of the present study's limitations are inherent to the pathology studied and the corresponding stimulation protocol. First, given the fact that the precentral and postcentral gyri were affected in 7% and 6% of cases, respectively, we cannot rule out the possibility that the NMA locations in these cases were distorted by the presence of the tumour. Moreover, the protocol for awake mapping during glioma surgery differs from that of extraoperative evaluation in epilepsy surgery (Mikuni *et al.*, 2006; Borggraefe *et al.*,

2016). To avoid after-discharges and seizures and reduce operating time, we did not increase the stimulation intensity after the threshold had been established. This method has proven its effectiveness in reducing the incidence of intraoperative seizures and in optimizing functional outcomes and the extent of resection (Duffau *et al.*, 2003; Boetto *et al.*, 2015). This difference in intensity level might explain the lack of NMRs over the inferior frontal gyrus or the rostral premotor areas (Mikuni *et al.*, 2006; Borggraefe *et al.*, 2016).

Differences in stimulation protocol between our present work and literature studies of NMRs complicate a direct comparison of the results. The current density in our study might have been higher than in the literature because of a smaller electrode surface area, with a greater risk of current diffusion to subcortical fibres. However, cortical stimulation is more focal because the lower inter-electrode distance decreases the edge-effect (Nathan *et al.*, 1993). Nevertheless, if subcortical current diffusion had been responsible for false-positives, we should have found NMRs at locations that had never before been described; this was not the case.

Interestingly, the spatial distribution of anatomical sites over the precentral gyrus observed here was quite similar to those in previous studies of smaller numbers of patients but with different protocols (Mikuni *et al.*, 2006; Borggraefe *et al.*, 2016). Even though NMRs were elicited by a lower intensity here, it is likely that the main NMAs are located in the precentral gyrus. The other NMAs observed on the lateral face of the hemisphere might belong to high-order areas, which would be connected to the core NMAs and constitute an input gate for the negative motor network (Mandonnet *et al.*, 2009). These results are consistent with the fact that some studies using subdural electrodes did not find any NMRs on rostral premotor areas either (Mikuni *et al.*, 2006; Enatsu *et al.*, 2013).

One further issue is whether the type of elicited response depends on the stimulation protocol (Mikuni *et al.*, 2006). In the present study, we did not increase the stimulation intensity; as a consequence, some PMR sites located in the same position as NMR sites might have been ignored. However, PMRs that occur at higher intensity might be due to a current diffusion to the PMA. Even though our study's stimulation parameters might have modified the nature of the response (NMR versus PMR) and thus the mapping, our results were very reproducible from one patient to another and with regard to other studies (Mikuni *et al.*, 2006; Enatsu *et al.*, 2013; Tate *et al.*, 2014; Borggraefe *et al.*, 2016). Furthermore, the existence of cortical NMRs is relevant, given the existence of subcortical NMRs (responses that cannot be converted into PMRs by increasing the intensity). Moreover, the glioma resection protocol used in the present study is a common, standard procedure (Duffau, 2004; Szelényi *et al.*, 2010); hence, our probabilistic map will probably reflect the 'real-life' clinical results that surgeons will obtain during surgery. Time constraints prevented us from assessing an NMR in detail (for example, asking the patient to move the tongue after a speech arrest, or specifically moving the fingers after an upper limb NMR). Accordingly, we cannot rule out the possibility that we underestimated the full extent of the NMRs. Further research is needed to tackle this issue. Next, some NMAs could have been missed because the surgery did not expose the entire cortical surface. Hence, our probabilistic map will having to be updated by adding new stimulation sites in other patients.

Lastly, we failed to show a difference between left and right-handers for cluster C—probably because there were few left-handers in our cohort: in future studies, this hypothesis will be checked by increasing the number of investigating sites.

Conclusion

The present report describes the largest series to date of patients presenting NMRs during electrical brain mapping. Our unique probabilistic map shows that NMAs are clustered and not randomly distributed. The NMAs appear to be part of a complex, large-scale, corticosubcortical subnetwork involved in motor control. Better knowledge of the NMAs' cortical distribution and their underlying connectivity might be useful for neurosurgeon-patient discussions, surgical planning, and intraoperative brain mapping in the fields of tumour and epilepsy surgery. Our map might also facilitate the prediction of motor recovery after brain damage and guide the rehabilitation process. Lastly, the map might help to understand the pathophysiology of movement disorders—perhaps by enabling the definition of new targets for brain stimulation. In addition to the map's clinical value, a better understanding of the negative motor network's functional anatomy might help neuroscientists to refine neurocognitive models of movement and to identify new regions of interest for functional neuroimaging. In summary, our probabilistic map represents a solid basis for further clinical and fundamental studies of motor control.

Acknowledgements

Data were provided by the Human Connectome Project, the WU-Minn Consortium (Principal Investigators: David Van Essen and Kamil Ugurbil; 1U54MH091657, funded by the 16 NIH Institutes and Centers that support the NIH Blueprint for Neuroscience Research), and the McDonnell Center for Systems Neuroscience at Washington University.

Funding

This research did not receive any specific grant from funding agencies in the public, commercial, or not-for-profit sectors.

Competing interests

The authors declare no competing interests.

Supplementary material

Supplementary material is available at *Brain* online.

References

Almairac F, Herbet G, Moritz-Gasser S, Duffau H. Parietal network underlying movement control: disturbances during subcortical electrostimulation. Neurosurg Rev 2014; 37: 513–6; discussion 516–7.

Ariani G, Wurm MF, Lingnau A. Decoding internally and externally driven movement plans. J Neurosci 2015; 35: 14160–71.

Boetto J, Bertram L, Moulinié G, Herbet G, Moritz-Gasser S, Duffau H. Low rate of intraoperative seizures during awake craniotomy in a prospective cohort with 374 supratentorial brain lesions: electrocorticography is not mandatory. World Neurosurg 2015; 84: 1838–44.

Boetto J, Bertram L, Moulinié G, Herbet G, Moritz-Gasser S, Duffau H. Electrocorticography is not necessary during awake brain surgery for gliomas. World Neurosurg 2016; 91: 656–7.

Borggraefe I, Catarino CB, Rémi J, Vollmar C, Peraud A, Winkler PA, et al. Lateralization of cortical negative motor areas. Clin Neurophysiol 2016; 127: 3314–21.

Bradnam LV, Stinear CM, Byblow WD. Ipsilateral motor pathways after stroke: implications for non-invasive brain stimulation. Front Hum Neurosci 2013; 7: 184.

Buccino G, Binkofski F, Riggio L. The mirror neuron system and action recognition. Brain Lang 2004; 89: 370–6.

Catani M, Dell'Acqua F, Vergani F, Malik F, Hodge H, Roy P, et al. Short frontal lobe connections of the human brain. Cortex 2012; 48: 273–91.

Cattaneo L, Rizzolatti G. The mirror neuron system. Arch Neurol 2009; 66: 557.

Chauvel PY, Rey M, Buser P, Bancaud J. What stimulation of the supplementary motor area in humans tells about its functional organization. Adv Neurol 1996; 70: 199–209.

Chouinard PA, Paus T. The primary motor and premotor areas of the human cerebral cortex. Neurosci Rev J Bringing Neurobiol Neurol Psychiatry 2006; 12: 143–52.

Davies DL, Bouldin DW. A cluster separation measure. IEEE Trans Pattern Anal Mach Intell 1979; 1: 224–7.

De Benedictis A, Moritz-Gasser S, Duffau H. Awake mapping optimizes the extent of resection for low-grade gliomas in eloquent areas. Neurosurgery 2010; 66: 1074–84.

Duffau H. Cartographie fonctionnelle per-opératoire par stimulations électriques directes: Aspects méthodologiques. Neurochirurgie 2004; 50: 474–83.

Duffau H, Capelle L, Denvil D, Sichez N, Gatignol P, Taillandier L, et al. Usefulness of intraoperative electrical subcortical mapping during surgery for low-grade gliomas located within eloquent brain regions: functional results in a consecutive series of 103 patients. J Neurosurg 2003; 98: 764–78.

Duffau H, Capelle L, Sichez JP, Faillot T, Abdennour L, Law Koune JD, et al. Intra-operative direct electrical stimulations of the central nervous system: the Salpetriere experience with 60 patients. Acta Neurochir (Wien) 1999; 141: 1157–67.

Duffau H, Mandonnet E. The "onco-functional balance" in surgery for diffuse low-grade glioma: integrating the extent of resection with quality of life. Acta Neurochir (Wien) 2013; 155: 951–7.

Dum RP. Frontal lobe inputs to the digit representations of the motor areas on the lateral surface of the hemisphere. J Neurosci 2005; 25: 1375–86.

Enatsu R, Matsumoto R, Piao Z, O'Connor T, Horning K, Burgess RC, et al. Cortical negative motor network in comparison with sensorimotor network: a cortico-cortical evoked potential study. Cortex 2013; 49: 2080–96.

Filevich E, Kühn S, Haggard P. Negative motor phenomena in cortical stimulation: implications for inhibitory control of human action. Cortex 2012; 48: 1251–61.

Glasser MF, Coalson TS, Robinson EC, Hacker CD, Harwell J, Yacoub E, et al. A multi-modal parcellation of human cerebral cortex. Nature 2016; 536: 171–8.

He SQ, Dum RP, Strick PL. Topographic organization of corticospinal projections from the frontal lobe: motor areas on the lateral surface of the hemisphere. J Neurosci 1993; 13: 952–80.

Herbet G, Maheu M, Costi E, Lafargue G, Duffau H. Mapping neuroplastic potential in brain-damaged patients. Brain 2016; 139: 829–44.

Ius T, Angelini E, Thiebaut de Schotten M, Mandonnet E, Duffau H. Evidence for potentials and limitations of brain plasticity using an atlas of functional resectability of WHO grade II gliomas: towards a 'minimal common brain'. NeuroImage 2011; 56: 992–1000.

Kinoshita M, de Champfleur NM, Deverdun J, Moritz-Gasser S, Herbet G, Duffau H. Role of fronto-striatal tract and frontal aslant tract in movement and speech: an axonal mapping study. Brain Struct Funct 2015; 220: 3399–412.

Kraskov A, Dancause N, Quallo MM, Shepherd S, Lemon RN. Corticospinal neurons in macaque ventral premotor cortex with mirror properties: a potential mechanism for action suppression? Neuron 2009; 64: 922–30.

Lüders H, Lesser RP, Morris HH, Dinner DS. Negative motor responses elicited by stimulation of the human cortex. In: Wolf P, Dam M, Janz D, editors. Advances in epileptology. New York: Raven Press; 1987. p. 229–31.

Lüders HO, Dinner DS, Morris HH, Wyllie E, Comair YG. Cortical electrical stimulation in humans. The negative motor areas. Adv Neurol 1995; 67: 115–29.

Makris N, Kennedy DN, McInerney S, Sorensen AG, Wang R, Caviness VS, et al. Segmentation of subcomponents within the superior longitudinal fascicle in humans: a quantitative, in vivo, DT-MRI study. Cereb Cortex 2005; 15: 854–69.

Mandonnet E, Jbabdi S, Taillandier L, Galanaud D, Benali H, Capelle L, et al. Preoperative estimation of residual volume for WHO grade II glioma resected with intraoperative functional mapping. Neuro Oncol 2007; 9: 63–9.

Mandonnet E, Winkler PA, Duffau H. Direct electrical stimulation as an input gate into brain functional networks: principles, advantages and limitations. Acta Neurochir (Wien) 2009; 152: 185–93.

Marcus DS, Harwell J, Olsen T, Hodge M, Glasser MF, Prior F, et al. Informatics and data mining tools and strategies for the human connectome project. Front Neuroinform 2011; 5: 4.

Martino J, Witt Hamer PC, Berger MS, Lawton MT, Arnold CM, Lucas EM, et al. Analysis of the subcomponents and cortical terminations of the perisylvian superior longitudinal fasciculus: a fiber dissection and DTI tractography study. Brain Struct Funct 2013; 218: 105–21.

Metz-Lutz M, Kremin H, Deloche G. Standardisation d'un test de de´ nomination orale: contro○ le des effets de l'a○ ge, du sexe et du niveau de scolarite´ chez les sujets adultes normaux. Rev Neuropsychol 1991: 73–95.

Mikuni N, Ohara S, Ikeda A, Hayashi N, Nishida N, Taki J, et al. Evidence for a wide distribution of negative motor areas in the perirolandic cortex. Clin Neurophysiol 2006; 117: 33–40.

Nathan SS, Sinha SR, Gordon B, Lesser RP, Thakor NV. Determination of current density distributions generated by electrical stimulation of the human cerebral cortex. Electroencephalogr Clin Neurophysiol 1993; 86: 183–92.

Penfield W, Boldrey E. Somatic motor and sensory representation in the cerebral cortex of man as studied by electrical stimulation, Brain 1937; 60: 389.

Pool E-M, Rehme AK, Eickhoff SB, Fink GR, Grefkes C. Functional resting-state connectivity of the human motor network: differences between right- and left-handers. NeuroImage 2015; 109: 298–306.

Rech F, Duffau H, Pinelli C, Masson A, Roublot P, Billy-Jacques A, et al. Intraoperative identification of the negative motor network during awake surgery to prevent deficit following brain resection in premotor regions. Neurochirurgie 2017; 63: 235–42.

Rech F, Herbet G, Moritz-Gasser S, Duffau H. Disruption of bimanual movement by unilateral subcortical electrostimulation. Hum Brain Mapp 2014; 35: 3439–45.

Rech F, Herbet G, Moritz-Gasser S, Duffau H. Somatotopic organization of the white matter tracts underpinning motor control in humans: an electrical stimulation study. Brain Struct Funct 2016; 221: 3743–53.

Rizzolatti G, Sinigaglia C. The mirror mechanism: a basic principle of brain function. Nat Rev Neurosci 2016; 17: 757–65.

Rousseeuw PJ. Silhouettes: a graphical aid to the interpretation and validation of cluster analysis. J Comput Appl Math 1987; 20: 53–65.

Schucht P, Moritz-Gasser S, Herbet G, Raabe A, Duffau H. Subcortical electrostimulation to identify network subserving motor control. Hum Brain Mapp 2013; 34: 3023–30.

Szelényi A, Bello L, Duffau H, Fava E, Feigl GC, Galanda M, et al. Intraoperative electrical stimulation in awake craniotomy: methodological aspects of current practice. Neurosurg Focus 2010; 28: 7.

Takahashi K, Best MD, Huh N, Brown KA, Tobaa AA, Hatsopoulos NG. Encoding of both reaching and grasping kinematics in dorsal and ventral premotor cortices. J Neurosci 2017; 37: 1733–46.

Takeuchi N, Chuma T, Matsuo Y, Watanabe I, Ikoma K. Repetitive transcranial magnetic stimulation of contralesional primary motor cortex improves hand function after stroke. Stroke 2005; 36: 2681–86.

Tate MC, Herbet G, Moritz-Gasser S, Tate JE, Duffau H. Probabilistic map of critical functional regions of the human cerebral cortex: Broca's area revisited. Brain 2014; 137: 2773–82.

Van Essen DC, Ugurbil K, Auerbach E, Barch D, Behrens TEJ, Bucholz R, et al. The human connectome project: a data acquisition perspective. NeuroImage 2012; 62: 2222–31.

van Geemen K, Herbet G, Moritz-Gasser S, Duffau H. Limited plastic potential of the left ventral premotor cortex in speech articulation: evidence from intraoperative awake mapping in glioma patients. Hum Brain Mapp 2014; 35: 1587–96.